

A study of the interannual variability of ECMWF surface re-analysis meteorological fields over the Mediterranean Basin for the period 1979-1993

S. CASTELLARI⁽¹⁾ and R. ARCHETTI⁽²⁾

⁽¹⁾ ISAO-CNR - Istituto Nazionale di Geofisica, Bologna, Italy

⁽²⁾ DISTART, Università di Bologna - Bologna, Italy

(ricevuto il 9 Novembre 1998; revisionato il 28 Ottobre 1999; approvato il 3 Febbraio 2000)

Summary. — The analysis of the ECMWF re-analysis surface meteorological fields (wind velocity, air temperature, relative humidity and cloud cover) is conducted on the Mediterranean basin and in its four small areas, mainly focusing on the interannual fluctuations of these data. This analysis (times series of surface integrals and EOF) shows an outstanding interannual signal in all data. In general, sporadic anomalous events in wind speed can occur during the winter months, while those in air temperature can occur during the summer months. Then, by comparing to COADS, a general underestimation of the wind speed and a good agreement in the air temperature are found.

PACS 92.60.Ry – Climatology.

1. – Introduction

The present study deals with the analysis of surface meteorological data for the period 1979-1993 over the Mediterranean basin (Med), its two sub-basins, the Western Mediterranean (WMed) and the Eastern Mediterranean (EMed), and few selected areas into the Med. The Med is a semi-enclosed mid-latitude basin of increasing interest because of several ocean processes taking place: deep convection, water mass formation and strong mesoscale circulation signal (Robinson *et al.*, 1991). At the present time, few meteorological surface data extensive in time (more than a decade) and space (covering the whole basin) are available for studies over the Med: the operational data from meteorological forecast global models and the ship-of-opportunity data. The first group consists only of two main data-sets: the National Center for Environmental Prediction (NCEP) data and the European Centre for the Medium-Range Weather Forecasts (ECMWF) data. The NCEP and ECMWF centers produce global forecast fields by using a four-dimensional data assimilation system, which has a set of first guess fields as base for the integration of the observations into the analysis. Using a numerical weather prediction (NWP) model from a previous analysis, the first guess usually is a 6 or 12 hour forecast and carries

the information from all the past analyses forward in time. Then the first guess is dependent upon the correctness of the NWP model and it can have a bias as a consequence. These operational analyses can be affected by major changes in assimilation, analysis technique, models and use of the observations in the operational NWP center. All these possible deficiencies of the operational forecast fields forced both centers to carry out consistent re-analyses of the global atmospheric data. These re-analyses are carried out by a data assimilation system, which is optimized for the production of medium-range forecasts. These data, ECMWF and NCEP (analyses and re-analyses), have been used for studies of the atmosphere-ocean climate system and for forcing ocean models: for example, they have been used in the surface boundary conditions of several ocean models of the Med and its regional seas (Heburn, 1994, 1987; Roussenov *et al.*, 1995; Wu and Haines, 1996, 1998; Pinardi *et al.* 1997).

On the other hand, the Comprehensive Ocean Atmosphere Data Set (COADS) is the most extensive in time and space among the ship-of-opportunity data-sets. The science project which has created the COADS data (Woodruff *et al.*, 1987) has gathered several historical data sets in only one consistent format and has suggested the ship reports to follow the same quality control procedure. The COADS data have been statistically analyzed in order to remove the typical observational biases and now are available as monthly means in 1×1 degree boxes over the global oceans and also as raw individual observations. Recently, Garrett *et al.* (1993) and Gilman and Garrett (1994) and [11] have used the COADS for studying the interannual variability of the surface heat fluxes over the Med.

These data (NCEP, ECMWF and COADS) contain the typical observed quantities: wind velocity, sea surface temperature (SST), surface air temperature, cloud cover and derived quantities (heat and momentum fluxes).

The aim of this study is to analyze the ECMWF surface Re-Analysis (ERA) meteorological fields over the Med, in particular focusing on the interannual variability signal during the period 1979-1993, and to compare these fields to the COADS observational fields. Section 1 presents the introduction. Section 2 describes the data-sets used, sect. 3 shows the analysis procedure, sect. 4 presents the analysis of the ERA data, sect. 5 the EOF analysis and sect. 6 the ERA-COADS comparison. Finally, sect. 7 presents the conclusions.

2. – The data

The first data-set used is the ERA 6 hrs (0000, 0600, 1200 and 1800 UTC) covering the period from January 1st 1979 to December 31st 1993 with horizontal resolution of approximately 1.125° in longitude and 1.1213° in latitude (Gibson *et al.*, 1997). The fields available for this study are: the 10 m wind components (u , v), the 2 m air temperature (T_A), the mean sea level pressure (P_S), the 2 m dew-point temperature (T_D) and the cloud cover (C_C). The 2 m relative humidity (r) has been estimated from the P_S , T_A and T_D through the formula

$$(1) \quad r = 100 \times \frac{e_s(T_D)}{p - e_s(T_D)} \times \frac{P_S - e_s(T_A)}{e_s(T_A)},$$

where $e_s(T) = c_1 \times e^{c_2(T - T_0)/(T - c_3)}$ is the saturation vapor pressure at a temperature T (Tetens formula), $T_0 = 273.16$ is a reference temperature, c_1 (610.78), c_2 (17.269 for

$T \geq T_0$ and 21.875 for $T < T_0$) and c_3 (35.86 for $T \geq T_0$ and 7.66 for $T < T_0$) are constants.

The second data-set used is the COADS-UWM (Da Silva *et al.*, 1995) prepared as a collaborative project between the University of Wisconsin-Milwaukee (UWM) and the National Oceanographic Data Center (NOAA). These data are monthly means derived from the original COADS and analyzed on a 1-by-1-degree global grid. They have been corrected by reducing a wind speed bias due to an erroneous Beaufort equivalent scale, by quality controlling the cloud cover observations and by assigning clear weather to certain missing Present Weather observations. The COADS-UWM fields available are: the 10 m wind components, the sea level air temperature, the 10 m relative humidity and the cloud cover. All these COADS fields are from January 1st 1979 to December 31st 1993, except for the relative humidity, which is available only from January 1st 1979 to December 31st 1989.

Both data-sets have been interpolated on a 0.25 degree grid of the Med, which is the same used by Castellari (1996), Pinardi *et al.* (1997) and Castellari *et al.* (1998b) for their modeling studies. This has been done because the ERA data are used to estimate surface momentum and heat fluxes to force ocean models of the Med.

3. – Analysis procedure

The study is conducted by analyzing the ERA data over the Med, WMed and EMed. In addition, four different areas (termed as A, B, C and D) are selected, which are important areas of water mass formations (see fig. 1). In these areas the surface air-sea fluxes play an important role and their interannual variability can influence the water mass formation processes (Castellari *et al.*, 1998b).

Firstly, monthly fields and anomaly monthly fields of all data available have been calculated. The anomaly monthly fields are estimated by subtracting a climatological monthly mean, calculated over the fifteen years of data, to all the monthly fields. This procedure eliminates the seasonal cycle from the monthly fields. Finally, surface

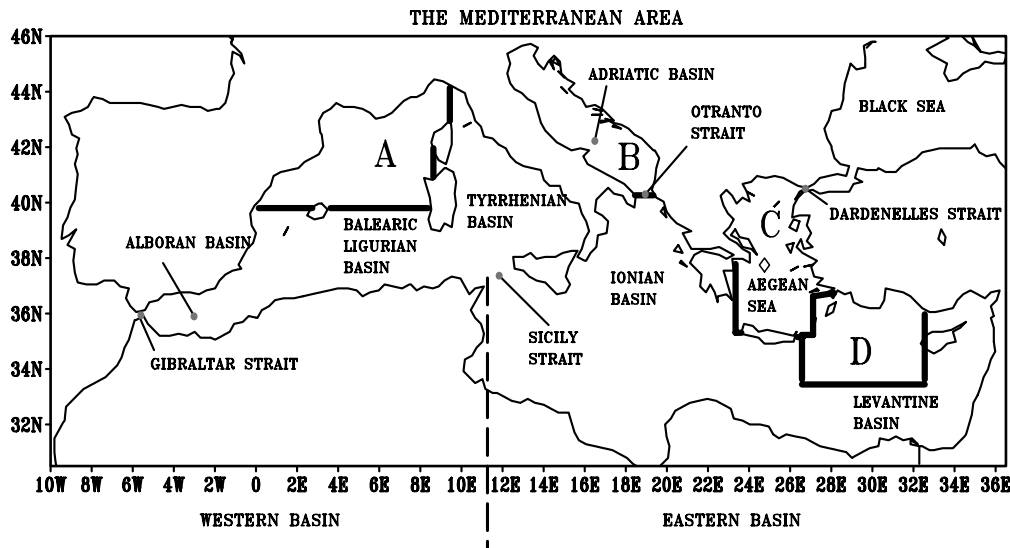


Fig. 1. – Mediterranean Sea nomenclature.

means of all monthly fields and anomaly monthly fields are estimated over the Med, WMed, EMed and the four selected areas.

Then, an Empirical Orthogonal Functions (EOF) analysis method (see appendix A) in the time domain to the ERA data has been applied in order to examine the spatial/temporal scales of the interannual variability of the ERA data. The EOF analysis has been used with the anomaly monthly fields. The first two modes spatial patterns and their associated amplitude time series (ATs) have been analyzed. Also a spectral analysis on the amplitude time series has been performed.

Since two independent data-sets (ERA and COADS) are available, a consistent comparison between them can be performed. The surface means of the ERA monthly fields and COADS fields over the Med have been compared by estimating their means, standard deviations, biases and round square mean errors (rmse) (see appendix B) and by means of scatterplots.

This comparison is concluded by comparing the interannual variability signal present in the ERA and in the COADS data. The "Interannual Anomaly Correlation Score" (IACS), which represents the horizontal correlation between two data-sets, is estimated from the anomaly monthly fields of ERA (*EA*) and COADS (*CA*) data. The IACS is given by

$$(2) \quad \text{IACS} = \frac{\text{Cor}(EA, CA)}{\sqrt{\text{Var}(EA) \cdot \text{Var}(CA)}} .$$

For a perfect correlation between the two fields the IACS is 1, and for the worst correlation the IACS is -1 .

4. – The analysis of ERA data

4.1. The Mediterranean basin. – The wind regime in the Med is prevalently northwesterly with the wind velocity *u*-components mostly positive and the wind velocity *v*-components mostly negative during the 1979-1993 period (not shown here). The anomaly wind speed signal shows the strongest wind events in January 1981, December 1981, January 1986, January 1987 and March 1988 (fig. 2A). The signal of the Etesian winds (northerly winds blowing on the Aegean and Levantine basins during summer) is not strong and is evident during the summer months from 1979 to 1985. Large negative anomalies in wind speed are present in January 1989, December 1984, December 1985, November 1989, January 1991 and January 1992 (fig. 2A). The strong wind event in January 1981 was found also by Heburn (1987) in his analysis of the interannual variability of the ECMWF 1000 mb data set used to force a model of the Med.

The anomaly air temperature signal shows large winter negative anomalies in March 1987 and December 1991, while it shows large winter positive ones in January 1988 and February 1990 (fig. 2B). Summer fluctuations are present: colder summers during 1979-1981, warmer summers during 1982-1984, followed by a colder summer in 1984 and warmer summers during 1985-1993, except for a colder summer in 1989. In general, the period from August 1987 to November 1990 is mostly characterized by large positive anomalies.

The relative humidity values present a range between 72% and 83% with a mean of about 77% (not shown here). The largest positive anomalies are in March 1981, November 1983 and March 1991, while the largest negative anomalies are in November

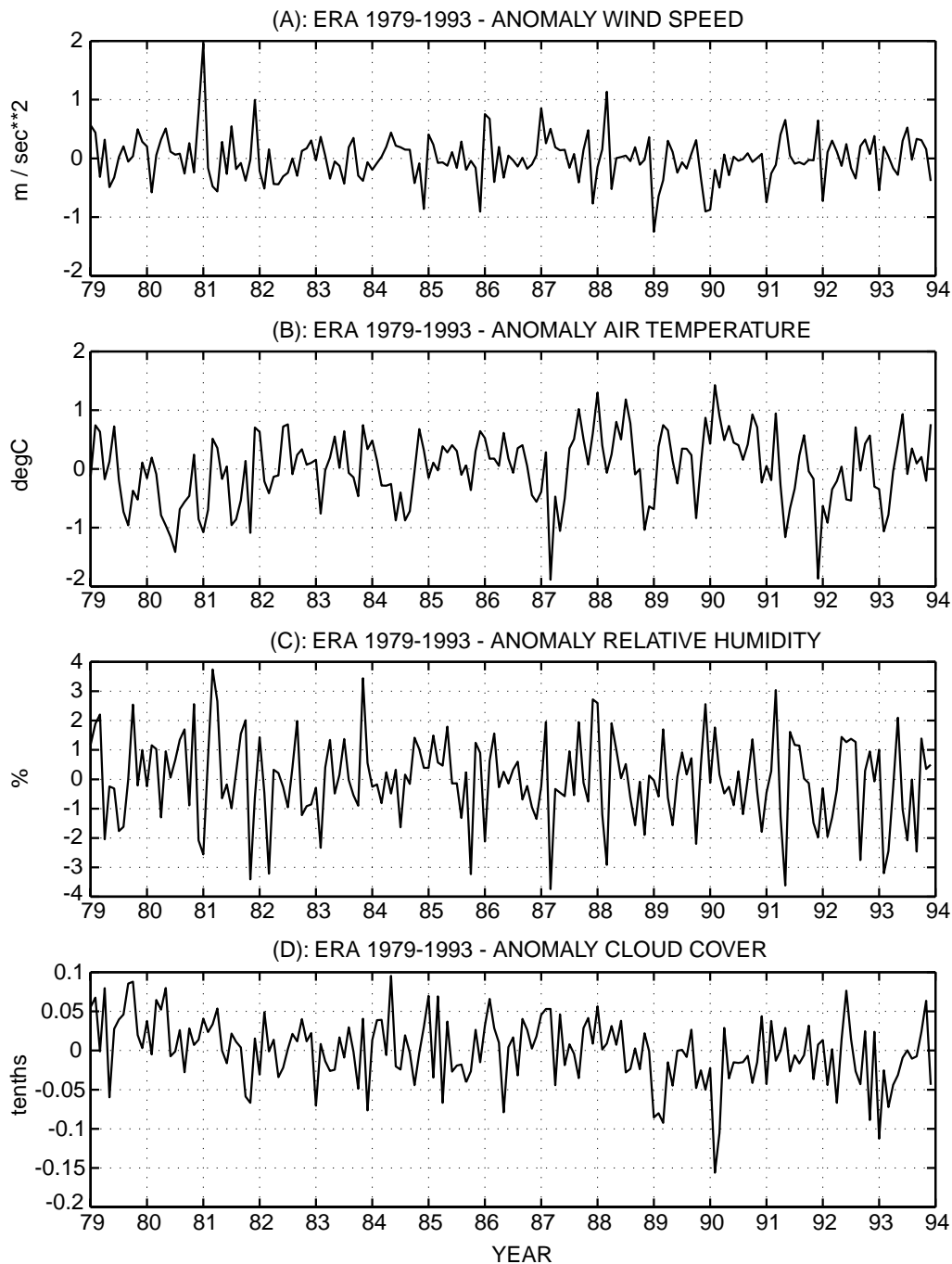


Fig. 2. – Med surface means of anomaly monthly ERA 1979-1993: anomaly wind speed (m/s) (A); anomaly air temperature ($^{\circ}\text{C}$) (B); anomaly relative humidity (%) (C); anomaly cloud cover (tenths) (D).

1981, March 1982, November 1985, February 1987, April 1991 and February 1993 (fig. 2C).

The cloud cover values range between 0 and 0.6 with a mean of 0.32 and the maximum value in January 1985 (not shown here). The anomaly cloud cover signal does not present large fluctuations (fig. 2D): it shows three large positive anomalies (October 1979, April 1984 and May 1992) and a large negative one (February 1990).

In general, in the decade 1980-1989 the year 1987 is the coldest one, followed by the years 1983 and 1981. The year 1981 is characterized by the coldest winter (with the strongest winds and low saturated air over the sea) and the coolest summer, while the year 1987 is characterized by a cold winter (with strong winds) and a hot summer.

Castellari *et al.* (1998a) have conducted a heat budget study over the Med by using the NCEP 12 hrs 1000 mb analysis data for the period 1980-1988 and they have found that the coldest year was the 1981. Besides, Castellari *et al.* (1998b), by investigating the interannual variability of the water mass formation processes in the Med, have shown strong Western Mediterranean Deep Water (WMDW) formation in the years 1981 and 1987.

Figure 3 shows the anomaly fields on the WMed and EMed. The wind speed, air temperature and cloud cover show the largest fluctuations over the WMed, while the relative humidity shows the largest one in the EMed. The wind speed shows the largest positive anomalies (over the WMed) in January 1981, December 1981, January 1986 and negative anomalies in December 1987 and January 1989 (fig. 3A). The largest positive anomalies of the air temperature are in January 1988 and February 1990 (over the WMed) and the largest negative anomalies are in August 1980, December 1980, August 1981, April 1991 (over the WMed), March 1987 and December 1991 (over the EMed) (fig. 3B). The anomaly relative humidity shows large positive anomalies in February 1980, October 1980, March 1981 and December 1993 and large negative anomalies in November 1981, November 1982, April 1991, October 1992 and October 1993 always over the EMed (fig. 3C). The anomaly cloud cover presents over the WMed the largest positive anomalies in October 1980, April 1984, February 1986 and the largest negative anomalies in January 1983, February 1990 and January 1993 (fig. 3D).

It is interesting to note that during the winter months of the 1987-1993 period the anomaly air temperature shows in the EMed larger negative anomalies than in the rest of the years. These cold air temperature values during the winter could be one of the factors responsible for exceptional Levantine Intermediate Water (LIW) and Levantine Deep water (LDW) formations in the Levantine Basin (Gertman *et al.*, 1987, 1994; Ozsoy *et al.*, 1993).

4.2. The area A. – Area A covers the Northern Balearic Ligurian basin, where the WMDW is formed during the winter months through a deep convection due to the intense surface cooling of the Mistral winds (MEDOC, 1970; Leman and Schott 1991; Schott *et al.*, 1993). These last studies have found evidence of deep convection, creating WMDW, in the Gulf of Lions during the winters of 1987 and 1991.

In the area A the largest values of wind speed are in January and December 1981, and in January 1986 (fig. 4A). The air temperature shows large minima in February 1981, January 1985, February 1986 and January 1987, while it shows maxima in the month of August of the years 1982, 1983, 1989, 1990 and 1992 (fig. 4B). It is possible to define three periods in the area A: a period 1979-1987 with cold winters except for the winter of 1982, a second period 1988-1990 with warm winters and a third period 1991-1993 again with cold winters. The relative humidity shows minima in January 1981, February 1984, February 1988 and July 1993, and large maxima in December 1987 and April 1988 (fig. 4C). The cloud cover signal has a mean of about 0.34 with large

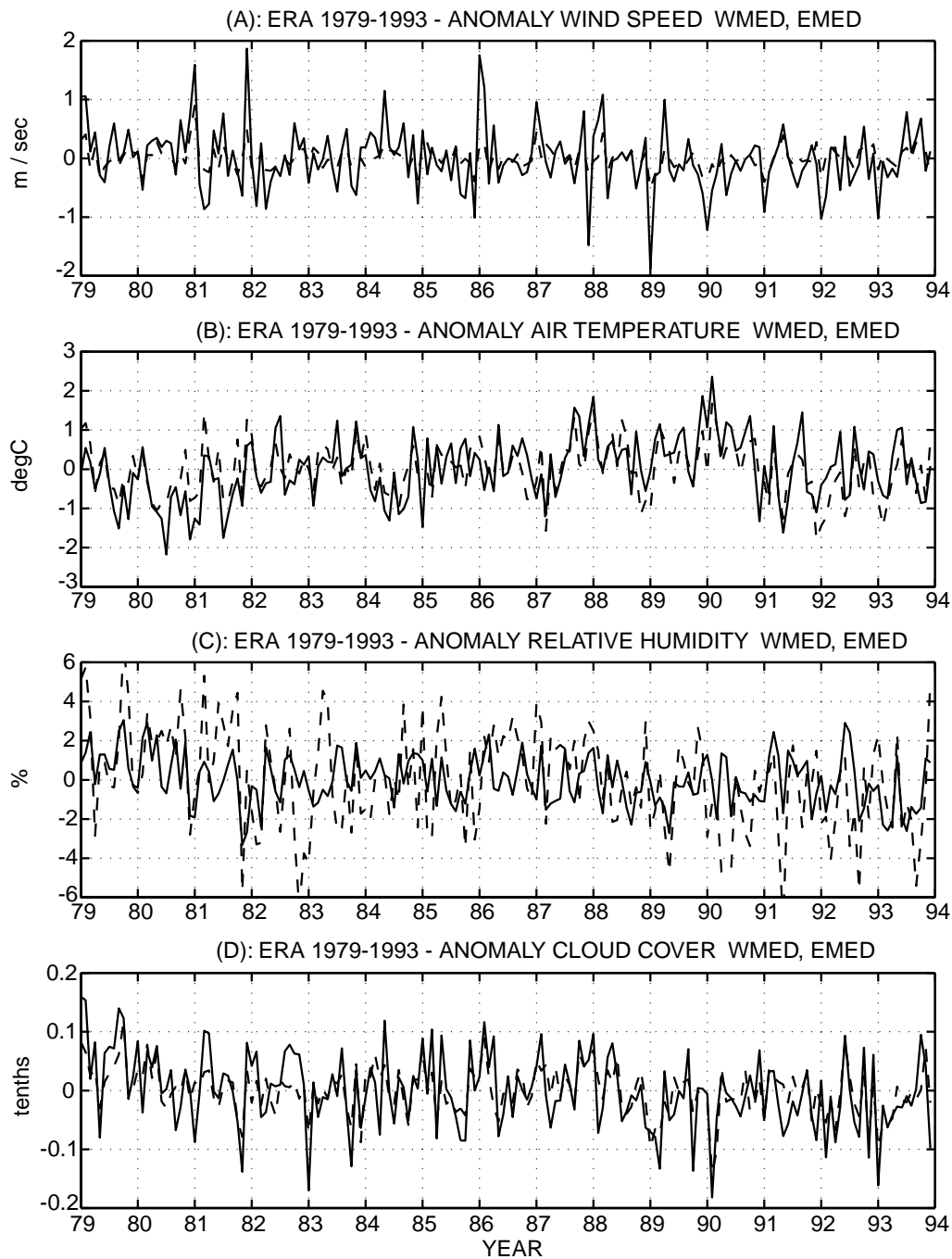


Fig. 3. – WMed (solid line) and EMed (dashed line) surface means of anomaly monthly ERA 1979-1993: wind speed (m/s) (A); air temperature (°C) (B); relative humidity (%) (C); cloud cover (tenths) (D).

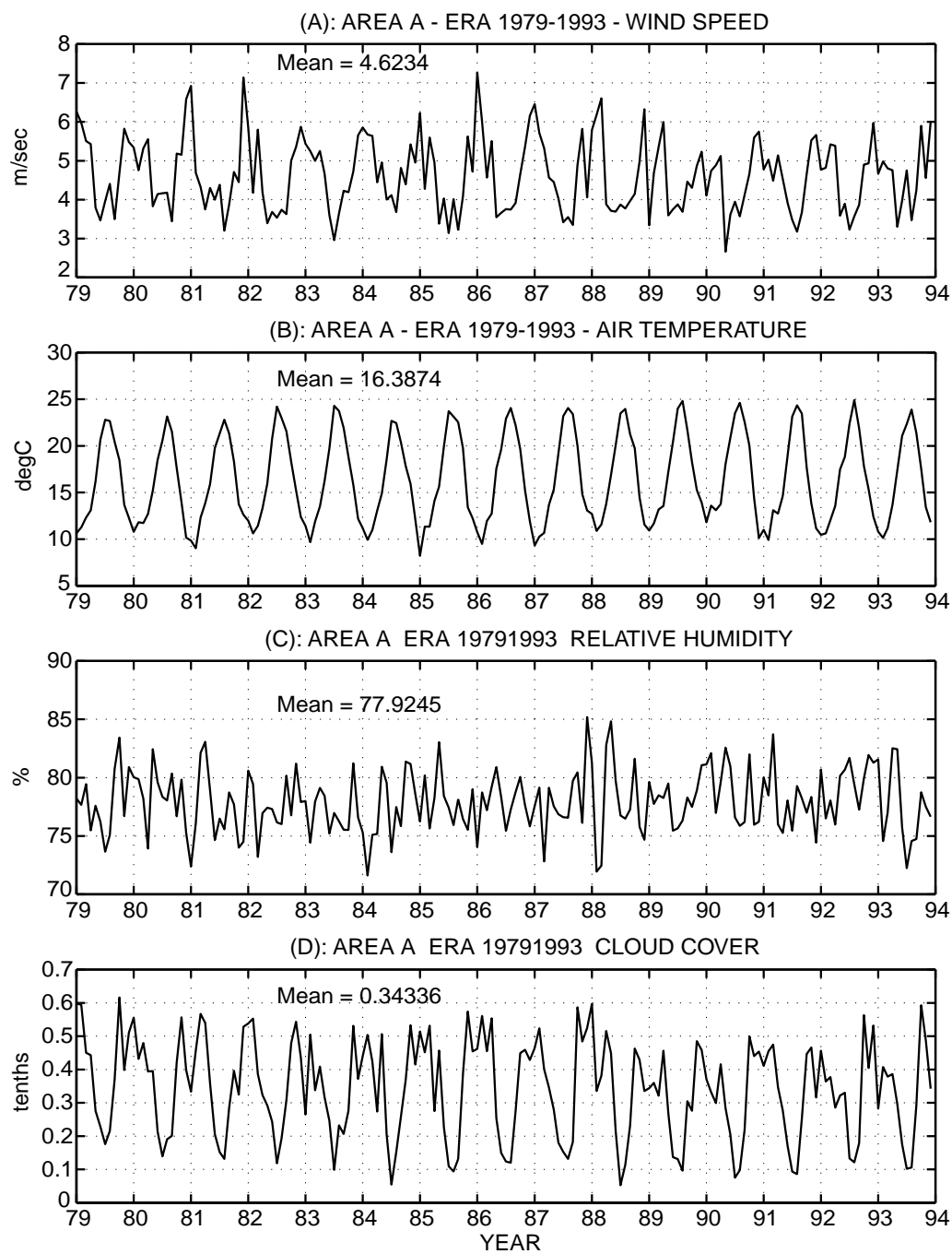


Fig. 4. – Surface means over the area A of ERA 1979-1993: wind speed /m/s (A); air temperature (°C) (B); relative humidity (%) (C); cloud cover (tenths) (D).

maxima in October 1979, October 1987, January 1988 and October 1993, while it shows minimum values in August 1984 and 1988 (fig. 4D). The maximum in wind speed in January 1987 followed by minima in air temperature and relative humidity in March 1987 is an indication that the 1987 winter has been particularly strong and characterized by strong wind and evaporation as found by Leaman and Schott (1991).

4.3. The area B. – Area B lies on the Adriatic basin, where the Adriatic Deep Water (ADW) is formed in its northern part and through a deep convective process in the southern part (Artegiani *et al.*, 1989, 1997). A large maximum in wind speed in January 1981 is correlated to a minimum of air temperature in the same time (fig. 5A, B). This correlation between a wind speed maximum and an air temperature minimum is present again only in December 1991 during the entire period 1979-1993. The other maxima in wind speed are in December 1983, December 1984 and January 1987. Besides the minimum in January 1981, the air temperature shows other minima in February 1983, February 1985, March 1987, December 1991 and February 1993 (fig. 5B). The maxima are in August 1988 and August 1992. The relative humidity shows a maximum in September 1982 and large minima in January 1981, February 1983, March 1987, December 1991, February 1992 and February 1993 (fig. 5C). The cloud cover signal shows large maxima in February 1984 and March 1986 (fig. 5D). It is possible to define three periods in this area by the analysis of the air temperature signal (fig. 5B): a 1979-1987 period with cold winters and warm summers, a 1988-1990 period with warm winters and warm summers and a 1991-1993 period again with cold winters and warm summers.

4.4. The area C. – Area C lies on the Aegean basin, which is the site of the formation of the Aegean Deep Water (AEDW) lately detected by Roether *et al.* (1996). They have found that the deep and bottom waters of the EMed have changed their characteristics in the year 1995: a large volume of deep and bottom water originating in the Aegean Sea has replaced part of the waters formed in the Adriatic Sea. They have suggested that changes in the circulation patterns or in the large-scale fresh water budget in the EMed since the year 1988 could have increased the salinity of the AEDW, which has affected the deep water formation in the area.

The wind speed signal presents a large maximum in December 1992, followed by other peaks in January 1987, February 1990 and December 1991 (fig. 6A). The summer months of the year 1979, 1988, 1989 and 1993 show very weak wind speed amplitude. The air temperature shows large minima in March 1987, February 1992 and January 1993, while it shows the largest maximum in July 1988 (fig. 6B). The relative humidity presents maxima in December 1983 and March 1991, while it shows large minima during the August 1984-1985, 1987-1988 and 1993 (fig. 6C). The cloud cover signal shows smaller values than in the previous areas with large maxima in January 1981, January 1984 and February 1986 (fig. 6D). The years 1987, 1992 and 1993 are found to be characterized by cold winters with strong wind events. It is possible to suggest that persistent anomalous large wind events can be responsible for large evaporation taking place in the Aegean Sea, and that the anomalous cold temperatures, following these wind events, could start the formation of intermediate and deep water with different characteristics than in the past.

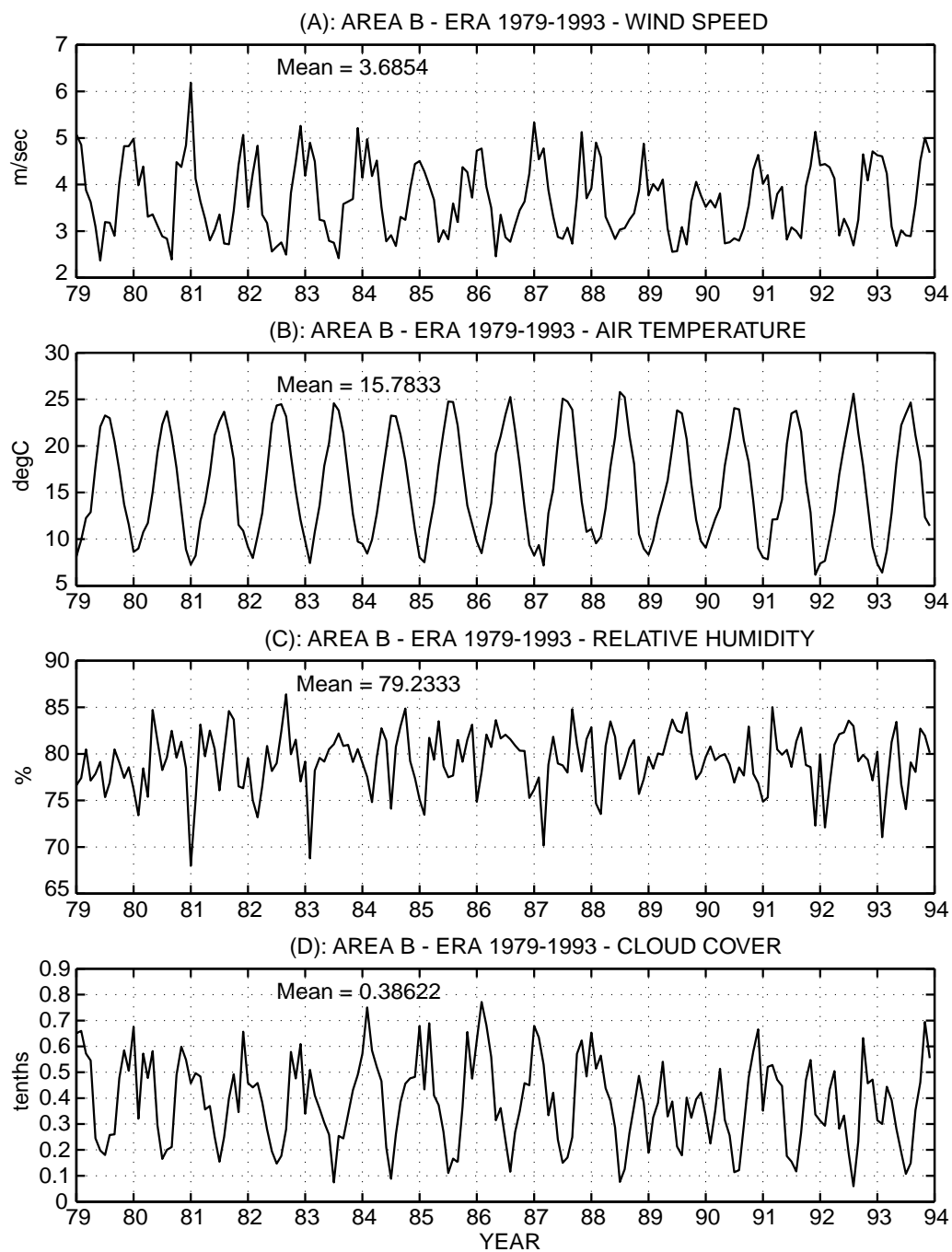


Fig. 5. – Surface means over the area B of ERA 1979-1993: wind speed (m/s) (A); air temperature (°C) (B); relative humidity (%) (C); cloud cover (tenths) (D).

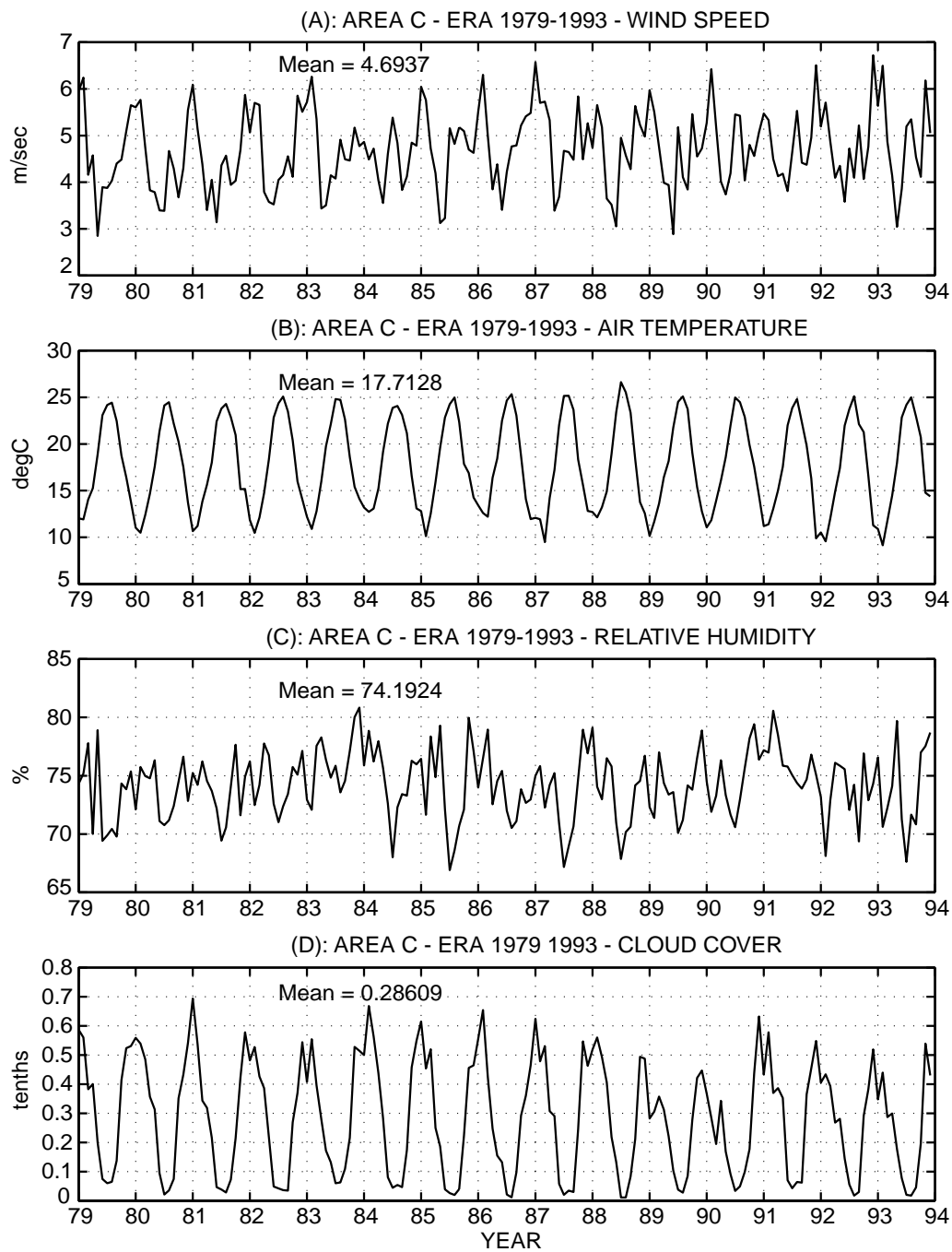


Fig. 6. – Surface means over the area C of ERA 1979-1993: wind speed (m/s) (A); air temperature (°C) (B); relative humidity (%) (C); cloud cover (tenths) (D).

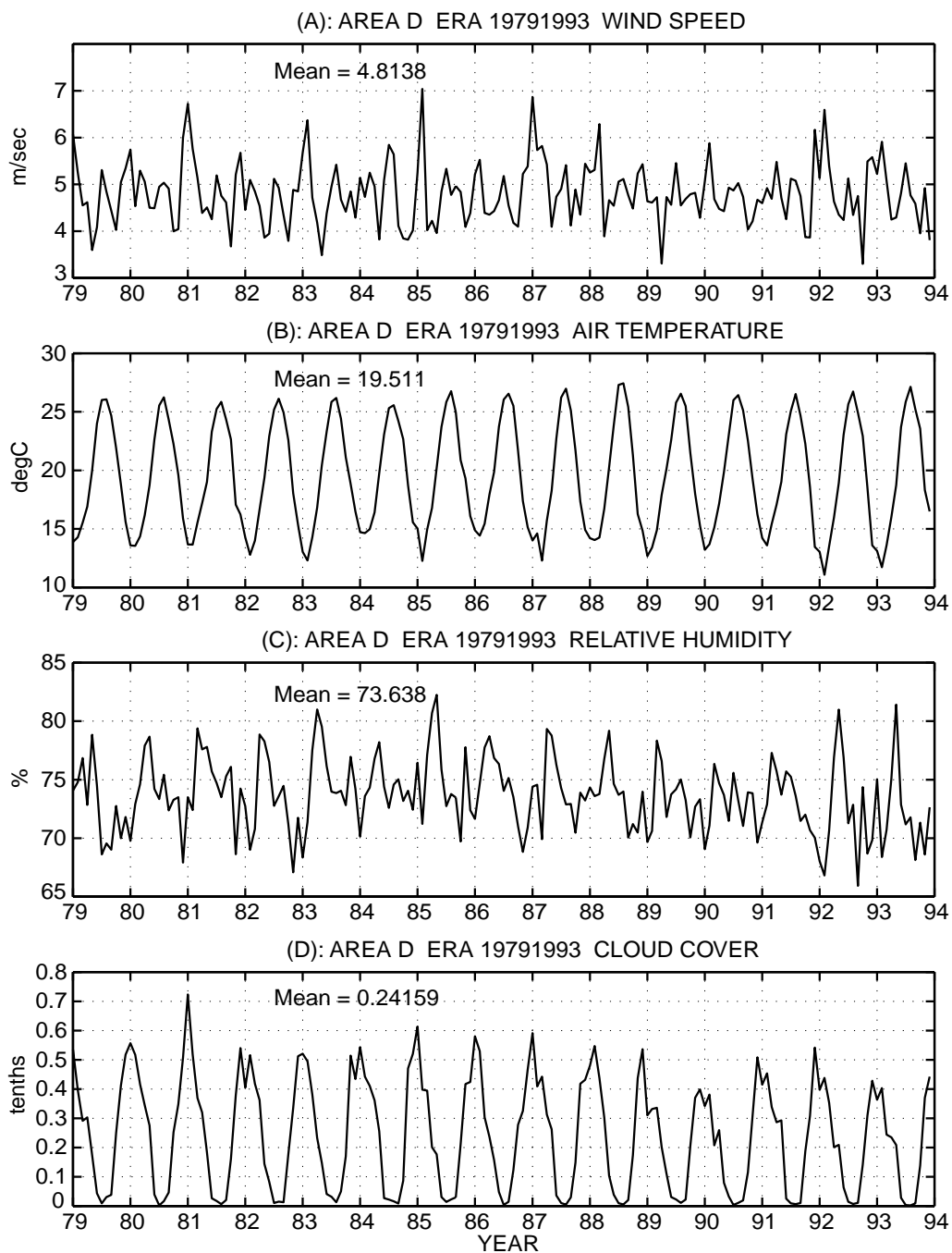


Fig. 7. – Surface means over the area D of ERA 1979-1993: wind speed (m/s) (A); air temperature (°C) (B); relative humidity (%) (C); cloud cover (tenths) (D).

4.5. *The area D.* – The area D is located in the Northern Levantine basin, which is the area of formation of the LIW by means of a mid-depth convection (Ovchinnikov, 1983; Hecht, 1986; Ozsay *et al.*, 1989; Robinson *et al.*, 1993; Lascaratos *et al.*, 1993) and of the LDW through a deep convection due to exceptionally cold winters. Recently, LDW formation has been detected in 1987 and 1990 (Gertman *et al.*, 1987; 1994) and in 1991 (Ozsay *et al.*, 1993) during winters characterized by cold air temperatures and strong winds.

The wind speed shows a maximum in February 1985, followed by secondary maxima in January 1981, February 1983, February 1985, January 1987 and February 1992 (fig. 7A). The minima in wind speed are in April 1983, March 1989 and November 1992. The wind speed maxima, except for that one in January 1981, are followed by large minima in the air temperature (fig. 7B). Furthermore, these anomalous events in air temperature and wind speed are followed by maxima in relative humidity in the month of April of 1983, 1985, 1992 and 1993 (fig. 7C). Finally, the cloud cover signal shows maxima in the month of January 1981, 1985 and 1987, while it does not show any relevant minimum (fig. 7D).

5. – The EOF analysis of the ERA data over the Mediterranean

We show the spatial patterns of the first two modes and their ATSs for the anomaly wind speed (fig. 8), anomaly air temperature (fig. 9), anomaly relative humidity (fig. 10) and anomaly cloud cover (fig. 11).

For the anomaly wind speed, the first two modes of the analysis explain 62% of the overall variability. The first ATS is characterized by spectral peaks at 3.0 and 0.9 years. This anomaly ATS shows a large positive peak of variability in December 1980 (fig. 8C), and large negative peaks in January 1989 and 1990. Inspection of the spatial pattern associated to the first EOF mode (fig. 8A) shows an in-phase oscillation of most of the basin with intensification in the Balearic-Ligurian and Tyrrhenian basins. Only the Aegean basin oscillates out of phase with the rest of the basin. On the other hand, the second spatial pattern (explaining 24% of the total variance) is characterized by the major part of the WMed oscillating out of phase with respect to the major part of the EMed. The center of maximum variability lies in the area south of the island of Crete (fig. 8B). The second ATS is characterized by spectral peaks at 1.7 and 0.8 years (fig. 8D).

The first two modes of the EOF analysis of the anomaly air temperature field explain 77% of the total variance. The spatial pattern associated to the first mode (fig. 9A) describes an in-phase oscillation of the whole basin with a meridional structure in most of the EMed and with a negative eastward amplitude gradient. The area of major intensification lies in the Alborean and Tyrrhenian basins. Spectral analysis of the first ATS shows the existence of periodicities of 3 and 1.2 years. This ATS shows the largest amplitudes of interannual variability in May 1980, May 1984, March 1987 and January 1992 (fig. 9C). On the other hand, the second EOF mode (explaining 22% of the total variance) shows a dipole (WMed and EMed out of phase) (fig. 9B). The largest signal lies in the Northern Balearic Ligurian and Northern Levantine basins. The ATS associated to the second anomaly mode shows strong intensification in March 1987, December 1988, November 1989, February 1992 and February 1993 (fig. 9D). This ATS is characterized by spectral peaks at 2.5 and 0.8 years. The EOF analysis shows the lack of sub-basin scales in the spatial patterns of the anomaly air temperature field.

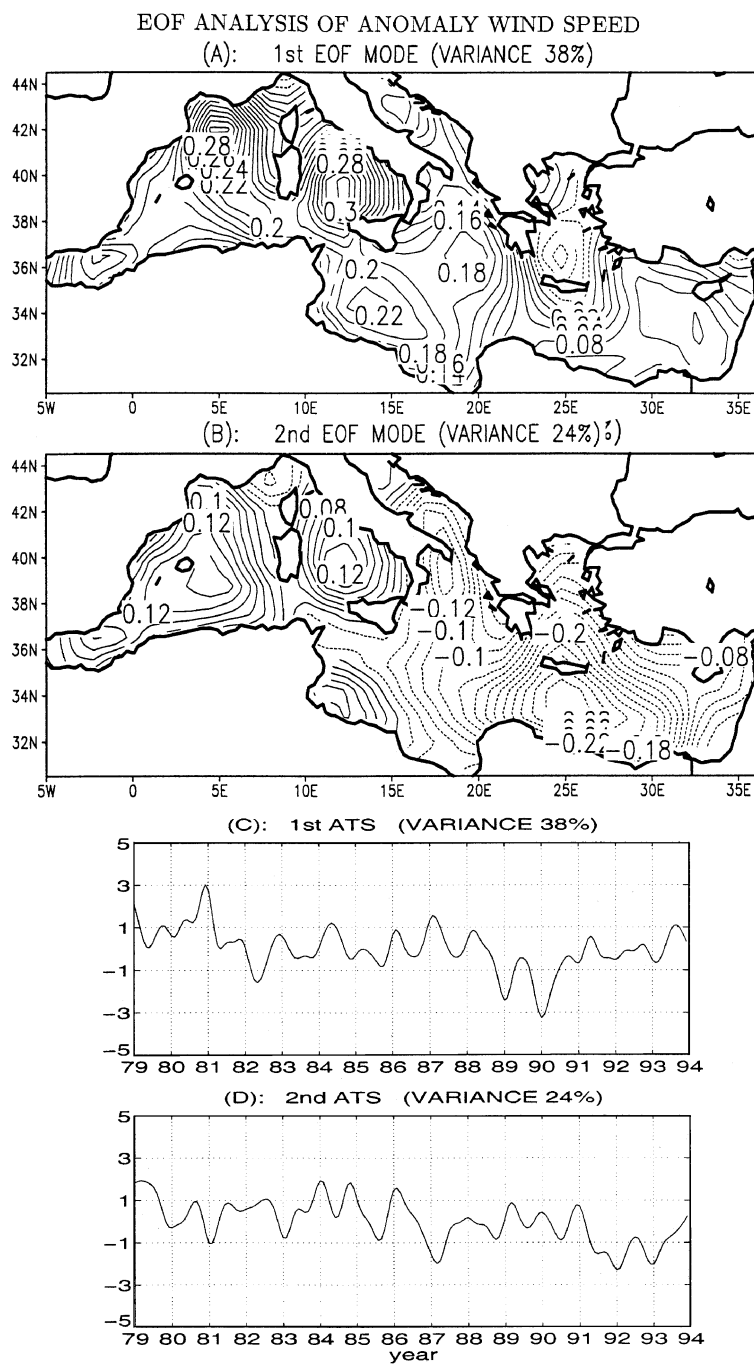


Fig. 8. – EOF analysis of ERA anomaly wind speed 1979-1993: 1st mode (A); 2nd mode (B); 1st ATS (C); 2nd ATS (D).

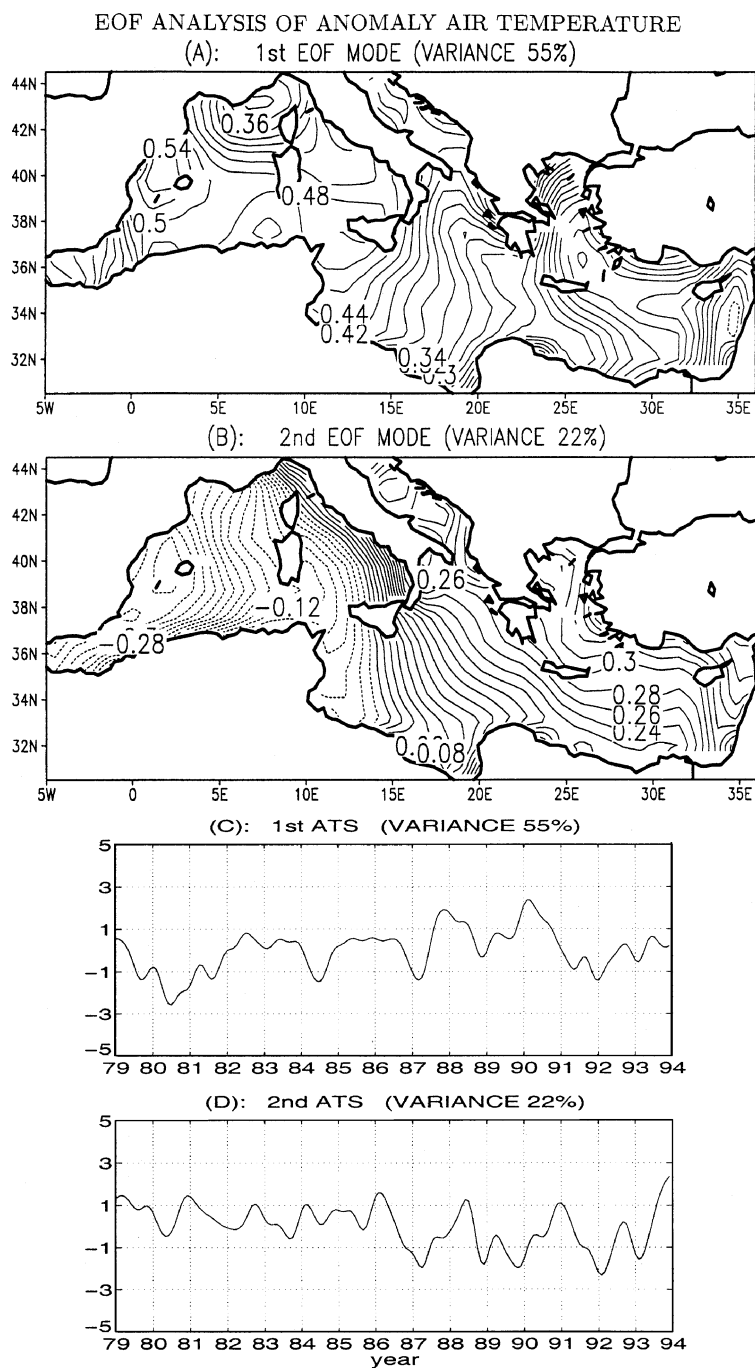


Fig. 9. – EOF analysis of ERA anomaly air temperature 1979-1993: 1st mode (A); 2nd mode (B); 1st ATS (C); 2nd ATS (D).

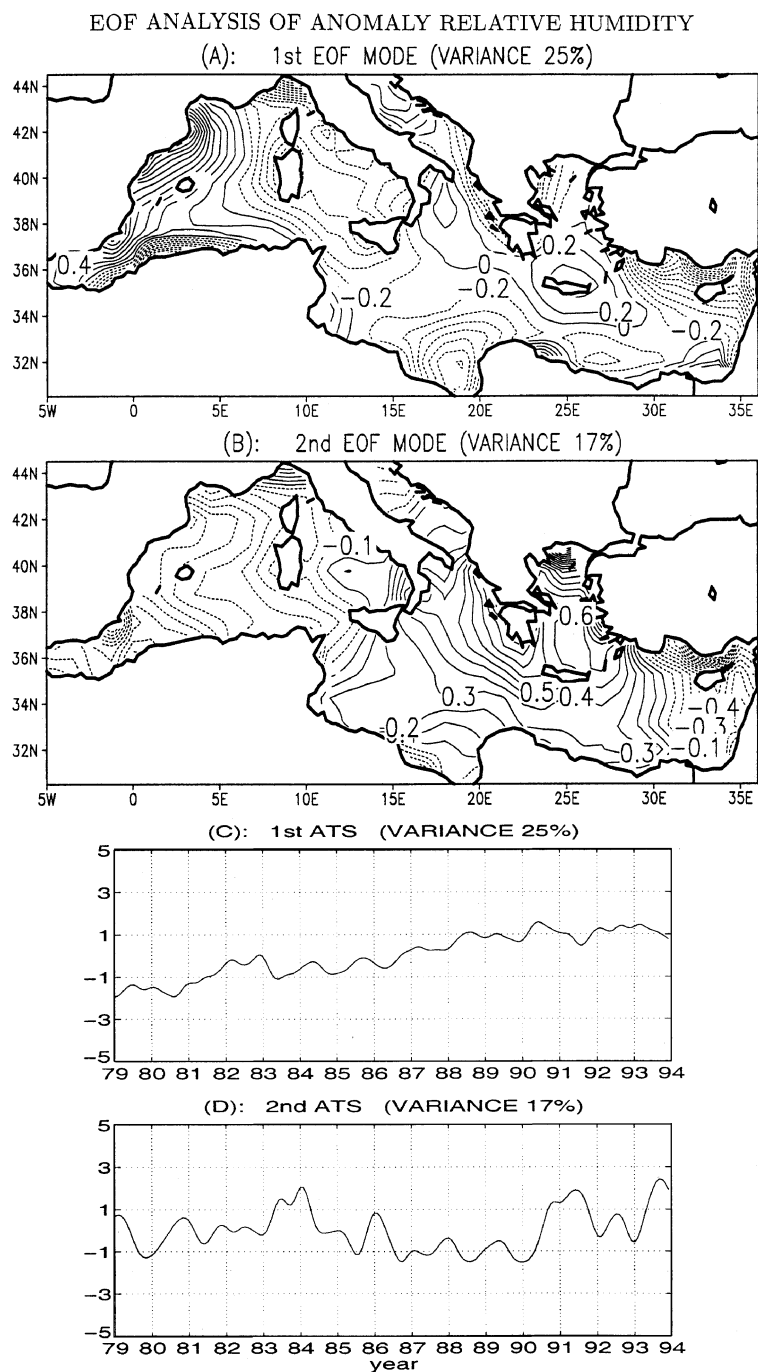


Fig. 10. – EOF analysis of ERA anomaly relative humidity 1979-1993: 1st mode (A); 2nd mode (B); 1st ATS (C); 2nd ATS (D).

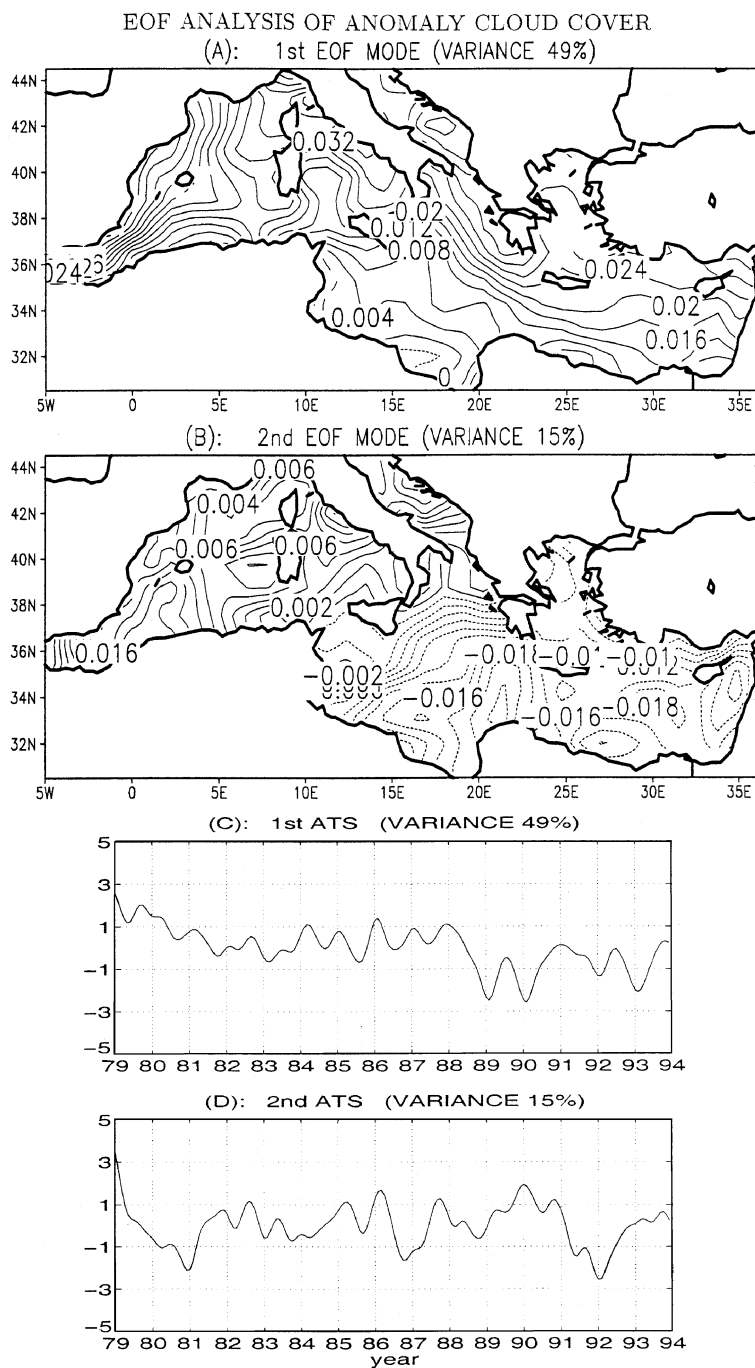


Fig. 11. – EOF analysis of ERA anomaly cloud cover 1979-1993: 1st mode (A); 2nd mode (B); 1st ATS (C); 2nd ATS (D).

For the anomaly relative humidity, the first two modes explain 42% of the overall variability. The first mode shows negative values in most of the basin except for the Gulf of Lions and the Northern Adriatic Sea (fig. 10A). The maxima are localized in the Aliborean basin and strong gradients are along the northern boundaries of the basin. The ATS associated to this first mode shows a trend of increasing amplitude as the time goes on (fig. 10C). For the second mode the WMed oscillates out of phase with respect to most of the EMed, except for the Northern Adriatic Sea and the Levantine basin (fig. 10B). The associated ATS presents large positive peaks of variability in January 1984, May 1991 and July 1993 (fig. 10D). Both ATSs have periodicities of 3 and 0.8 years.

The first and second modes of the anomaly cloud cover field explain 64% of the total variance. The first spatial patterns shows an in-phase oscillation of the overall basin with larger values in the WMed (fig. 11A). Its associated ATS shows a strong variability in the period 1988-1993 (fig. 11C) and presents spectral peaks at 3.7 and 0.9 years. On the other hand, a dipole over the basin is shown by the second spatial pattern, which oppose the EMed to the WMed and the Adriatic basin (fig. 11B). The associated ATS shows large peaks of variability in December 1980, February 1986, January 1990 and January 1992 (fig. 11D). There is only one spectral peak at 3 years.

In general, the EOF analysis of the ERA data shows that the first modes describe an in-phase oscillation of the whole basin, while the second ones describe a dipole (the WMed out of phase with the EMed). The study of ATSs of both modes shows a lock of interannual variability to the seasonal cycle since in most cases the amplitude time series intensifies during the early winter months (January-February).

6. – ERA-COADS comparison

Table I shows a statistical analysis of the ERA and COADS data. The velocity v -component and the relative humidity have positive biases on the means, while the velocity u -component has a negative bias and a larger rmse than the v -component. This means that the COADS and ERA present different orientations in the wind vectors, which would produce differences also in the estimation of the wind stress curl. The ERA wind speed is consistently underestimated with respect to the COADS wind speed, since the wind speed bias is -1.81 m/s. The air temperature and the relative humidity present biases of 0.39°C and of 1.81% .

The scatterplots of the monthly averaged surface means over the Med of each ERA *vs.* COADS field are shown in fig. 12. Again the ERA wind speed is underestimated with respect to the COADS wind speed (fig. 12C). The velocity u -component shows a weaker correlation than the velocity v -component (fig. 12A, B). The ERA air

TABLE I. – *Statistical analysis of ERA and COADS data.*

	ERA mean	ERA std	COADS mean	COADS std	Bias	rmse
u	1.07	0.77	1.29	0.93	-0.22	0.42
v	-1.02	0.68	-1.25	0.74	0.23	0.32
$ \vec{V} $	4.81	0.79	6.63	1.03	-1.81	1.84
T_A	18.62	4.49	19.01	4.33	-0.39	0.47
r	77.24	2.06	75.43	2.67	1.81	2.16
C	0.32	0.16	0.43	0.14	-0.1	0.12

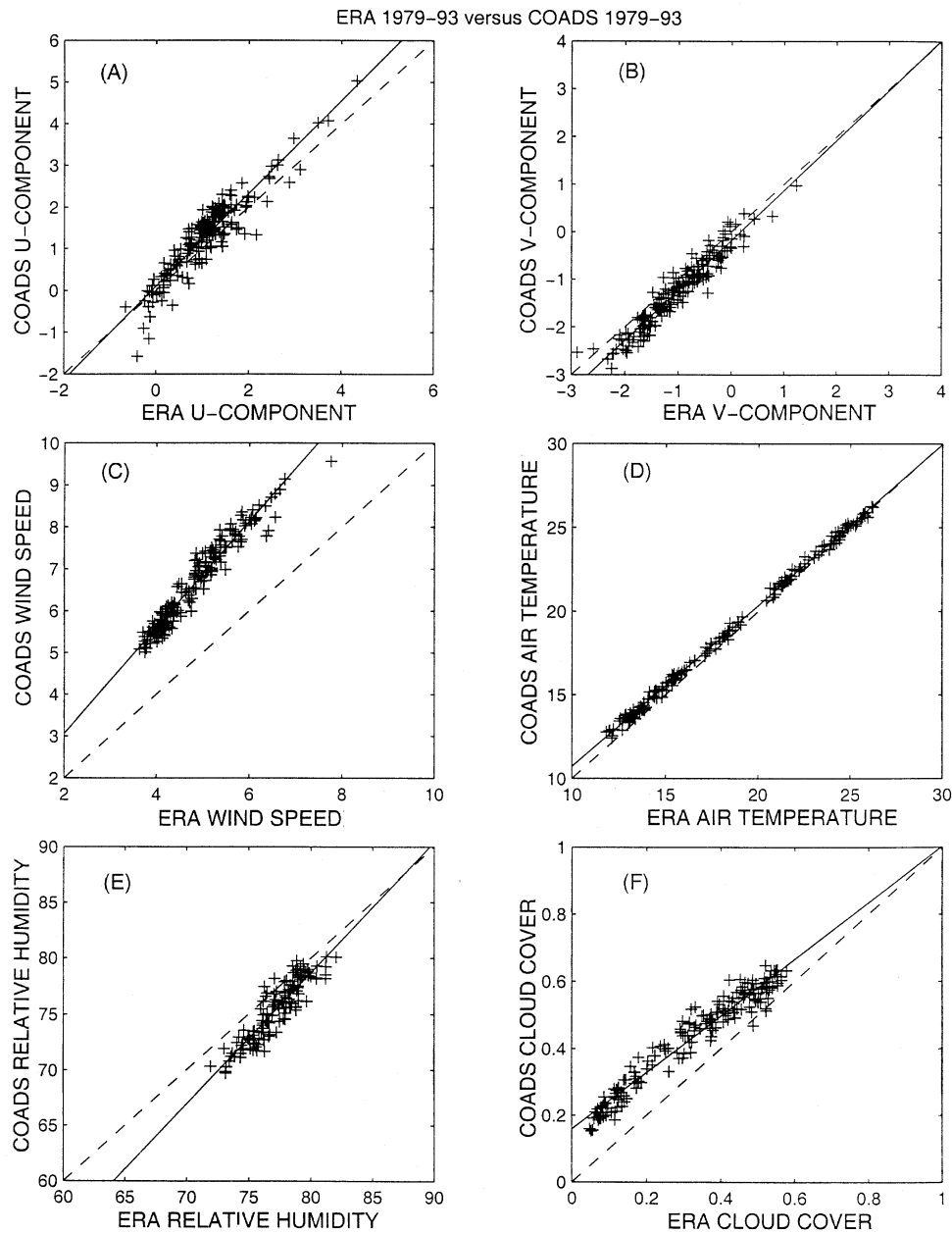


Fig. 12. – Scatterplots of Med surface means of ERA vs. COADS: wind velocity u -component (m/s) (A); wind velocity v -component (m/s) (B); wind speed (m/s) (C); air temperature (°C) (D); relative humidity (%) (E); cloud cover (tenths) (F).

temperature shows the best correlation with COADS (fig. 12D). The ERA relative humidity overestimates the COADS values (fig. 12E), while the ERA cloud cover shows a small underestimation with the COADS (fig. 12F).

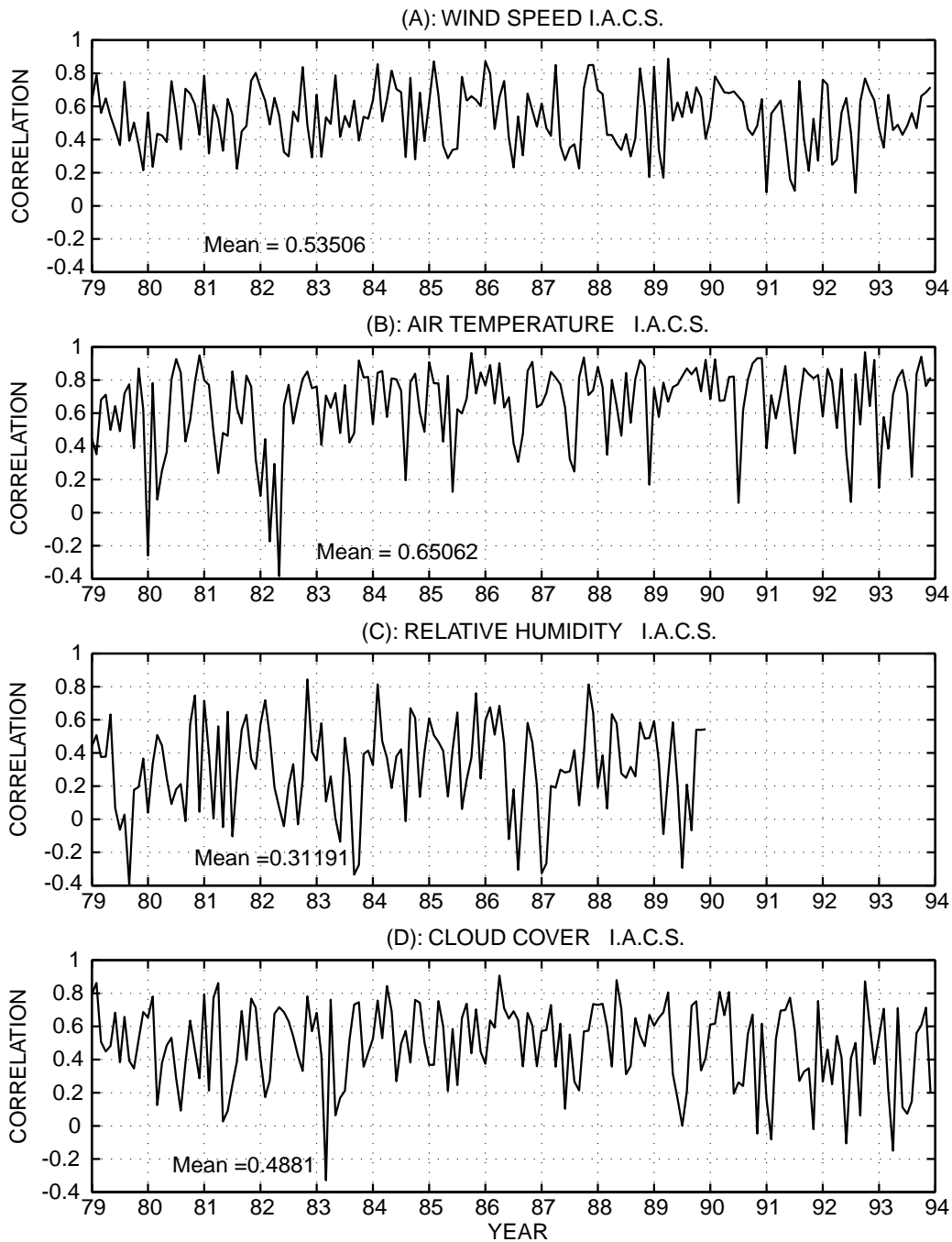


Fig. 13. – Interannual Anomaly Correlation Score (IACS) of ERA *vs.* COADS: wind speed (A); air temperature (B); relative humidity (C); cloud cover (D).

The means of the IACS of each variable are small: from about 0.31 for the relative humidity to about 0.65 for the air temperature. The ERA air temperature data are the best in reproducing the interannual anomalies of the COADS and show the best correlations during each Fall-Spring period (fig. 13B). In general, the ERA wind speed (fig. 13A) along with the relative humidity (fig. 13C) and the cloud cover (fig. 13D) show a weak correlation with COADS.

7. – Conclusions

An analysis of the ERA surface meteorological fields in the Med has been conducted focusing on the interannual fluctuations in the period 1979-1993. A large interannual variability signal of the ERA data has been shown in the Med and in four selected areas (important for the ocean processes taking place there). The wind speed has shown a salient peak in January 1981, which has been detected also by Castellari *et al.* (1998a) and Heburn (1987) by using different meteorological data. Also events of cold air temperature in March 1997 and December 1991 have been detected in the whole Med and they can have an effect on the water mass formation processes. The analysis of the air temperature signal over the Med during the summer (June-August) has allowed to define three main periods (1979-1981, 1982-1984 and 1985-1993) characterized by the intensity of the summer signal. In the area C (the Aegean basin) the years 1987, 1992 and 1993 are characterized by cold winters with strong wind events, which could be responsible for the change of the AEDW formed in that area. In the area D (Northern Levantine Basin) strong winds and cold air temperatures have been found in the month of January 1981 and 1987, and in the month of February 1983, 1985 and 1992. In the winter months of 1987 and 1992 Gertman *et al.* (1987) and Ozsoy *et al.* (1993) have shown these anomalous meteorological events being responsible for deep convective processes in the water mass formations in this area.

Then the EOF analysis method has been applied to the “interannual anomalies” of the meteorological fields over the whole Med and the first, the second mode and the associated ATSs have been studied. In general, the analysis on the wind speed has shown the first mode and ATS (38% of the variance) detecting large anomalies in January 1981, 1989 and 1990. The first mode and ATS (55% of the variance) of the air temperature have evidenced a cold period in 1980-1981 and a warm period in 1987-1990. Furthermore, the analysis of the relative humidity has shown an increasing trend in the first ATS (25% of the variance) and large anomalies in January 1984 and during the period 1991-1993 in the second ATS (17% of the variance).

Finally, a comparison of the monthly averaged ERA data to the COADS data has been performed. The ERA wind speed has been shown to be underestimated with respect to the observations, due mainly to the bias on the *u*-component. This bias can affect the possible estimation of the momentum fluxes needed to force ocean models of the Med. Cavaleri and Bertotti (1997) have analyzed the accuracy of the ERA winds on the Adriatic Sea by using them to force a wave model. They have found a general underestimate (20%-30%) of the significant wave height with respect to the observations. They have suggested a possible correction by enhancing the wind velocity of 50% for the Adriatic Sea. The biases on the wind velocity could depend on the inability of the ECMWF model at T106 resolution to simulate properly the strong gradients present in storms and the orography surrounding the several small sub-basins of the Med. This salient difference in the wind velocity between the ERA

and COADS data deserves further analysis. On the other hand, the ERA air temperature field is well correlated to the COADS, despite a bias on the mean of about -0.39°C . The other two remaining fields, the relative humidity and the cloud cover, do not show good agreement with the COADS. These ERA fields present problems in reproducing the COADS values and their interannual anomalies. Caution should be put on the validity of the ERA relative humidity, since it is a field hard to be simulated correctly by the operational models. On the other hand, the ERA cloud cover data should be considered more accurate than the COADS, which are visual estimates, since they can benefit from observations, satellite and elaborate radiation model.

Concluding, this study has permitted a tentative discussion on the general value of the ERA meteorological fields over the Med. In principle, these data can be a major resource for studies of climate and climate variability. However, we have confirmed that, for the Med at least, caution should be maintained in the usage of these data for forcing ocean models. Future work will involve estimation of the momentum and heat fluxes over the Med by means of updated bulk formulae of air-sea physics interaction.

APPENDIX A

Empirical Orthogonal Functions

The EOF analysis method has been introduced in a meteorological study by Lorenz (1956) and it has been used extensively in several studies in order to describe geophysical fields in meteorology, oceanography and hydrology (Weare *et al.*, 1976; Hardy and Walton, 1978, Salstein *et al.* 1983). It is an appropriate technique to derive the dominant variability patterns from a set of fields of any type. The temporal variability of the data can be expressed in orthogonal spatial patterns (EOF patterns), which are the eigenvectors of a scatter/covariance matrix. These eigenmodes are characterized by mutual orthogonality and by the efficiency to describe the initial field in the most economical way, since they reduce the dimensionality of the problem. When a set of orthogonal spatial modes is identified, the ordered successive eigenvectors can explain the maximum of the remaining variance of the data. A series of coefficients describing the time evolution of each spatial mode is associated to each eigenvector pattern. Because of this orthogonality, any two modes and their time variations are uncorrelated in space.

Mathematically, if $\gamma_j(x)$ is a time series of a 2D field, where $x = 1, \dots, m$ indicates the number of grid points and $j = 1, \dots, n$ indicates the number of time steps, we can write a matrix $d(x, t)$ containing the n -realizations of $\gamma_j(x)$. Then we can express $d(x, t)$ as

$$(A.1) \quad d(x, t) = \sum_{i=1}^r e_i(x) \lambda_i^{1/2} a_i(t),$$

where e_i are the EOF patterns, λ_i the eigenvalues and a_i the amplitude time series (ATS) of each EOF mode.

APPENDIX B

Statistics

Here we define the statistical parameters used in the study. The X_i and Y_i represent two time series and N is the number of samples.

Mean:

$$(B.1) \quad \bar{X} = \frac{1}{N} \sum X_i.$$

Standard deviation about the mean:

$$(B.2) \quad \sigma = \sqrt{\frac{1}{N-1} \sum (X_i - \bar{X})^2}.$$

Bias:

$$(B.3) \quad B = \bar{Y} - \bar{X}.$$

Root mean square error:

$$(B.4) \quad \text{RMSE} = \sqrt{\frac{1}{N} \sum (Y_i - X_i)^2}.$$

* * *

We appreciate the valuable assistance provided by Dr. E. SCHIANO (IOF-CNR, La Spezia, Italy), Dr. A. GRIFFA (IOF-CNR, La Spezia, Italy), Dr. J. M. BRANKART, (MEOM-LEGI, Grenoble, France) and Dr. N. PINARDI (University of Bologna, Italy).

REFERENCES

- ARTEGIANI A., AZZOLINI R. and SALUSTI E., *Oceanol. Acta*, **12** (1989) 151-160.
 ARTEGIANI A., BREGANT D., PASCHINI E., PINARDI N., RAICICH F. and RUSSO A., *J. Phys. Ocean.*, **27** (1997) 1492-1514.
 CASTELLARI S., PINARDI N. and LEAMAN K., *J. Marine Systems*, **18** (1998) 89-114.
 CASTELLARI S., PINARDI N. and LEAMAN K., to be published *J. Geophys. Res.*, **18** (2000).
 CASTELLARI S., Ph. D. dissertation, University of Miami, FL, USA (1996).
 CAVALERI L. and BERTOTTI L., *Monthly Weather Rev.*, **125** (1997) 1964-1975.
 DA SILVA A. M., YOUNG C. C. and LEVITUS S., *Atlas of Surface Marine Data 1994* (NOAA/National Oceanographic Data Center) 1995.
 GARRETT C., OUTERBRIDGE R. and THOMPSON K., *J. Climate*, **6** (1993) 900-910.
 GERTMAN I. F., POPOV Y. I. and TRIGUB V. G., Archived at Viniti, Moscow, No. 6581-B87.
 GERTMAN I. F., OVCHINNIKOV I. M. and POPOV Y. I., *Oceanology*, **34** (1994) 19-24.
 GIBSON J. K., KALLBERG P., UPPALA S., HERNANDEZ A., NOMURA A. and SERRANO E., ECMWF Re-Analysis Project Report Series, 1997.
 GILMAN C. and GARRETT C., *J. Geophys. Res.*, **99** (1994) 5119-5134.
 HARDY D. M. and WALTON J. J., *J. Appl. Meteorol.*, **17** (1978) 1153-1162.
 HEBURN G. W., *Coastal Estuarine Stud.*, **46** (1994) 249-285.
 HEBURN G. W., *Ann. Geophys. B*, **5** (1987) 61-74.

- HECHT A. N., in *Proceedings of the UNESCO/IOC Workshop on Physical Oceanography of the Eastern Mediterranean*, edited by A. R. ROBINSON and P. MALANOTTE RIZZOLI (Middle East Technical University, Erdemli, Turkey) 1986.
- LASCARATOS A., WILLIAMS R. G. and TRAGOU E., *J. Geophys. Res.*, **98** (1993) 14739-14749.
- LEAMAN K. and SCHOTT F. A., *J. Phys. Oceanogr.*, **21** (1991) 575-598.
- LORENZ E. N., in Technical Report, *Statistical Forecast Project Report 1* (Department of Meteorology, MIT, Boston, USA) 1956.
- MAGGIORE A., PINARDI N. and ZAVATARELLI M., in II Data Report PRISMA-II (Bologna, Italy) 1998.
- MEDOC GROUP, *Nature*, **227** (1970) 1037-1040.
- NITTIS K. and LASCARATOS A., *J. Marine Systems*, **18** (1997) 179-195.
- OVCHINNIKOV I. M., *Oceanology*, **23** (1983) 719-721.
- OZSOY E., HECHT A., UNLUATA U., BRENNER S., SUR H. I., BISHOP J., LATIF M. A., ROZENTRAUB Z. and OGUZ T., *Deep Sea Res.*, **40** (1993) 1075-1119.
- OZSOY E., HECHT A. and UNLUATA U., *Prog. Oceanogr.*, **22** (1989) 125-170.
- PINARDI N., KORRES G., LASCARATOS A., ROUSSENOV V. and STANEV E., *Geophys. Res. Lett.*, **24** (1997) 425-428.
- ROBINSON A. R., GOLNARAGHI M., LESLIE W. G., ARTEGANI A., HECHT A., LAZZONI E., MICHELATO A., SANSONE E., THEOCHARIS A. and UNLUATA U., *Dyn. Atm. Ocean.*, **15** (1991) 215-240.
- ROETHER W., MANCA B., KLEIN B., BREGANT D., GEORGIOPOULOS D., BEITZEL W., KOVACEVIC V. and LUCHETTA A., *Science*, **271** (1996) 333-334.
- ROUSSENOV V., STANEV E., ARTALE V. and PINARDI P., *J. Geophys. Res.*, **100** (1995) 13515-13538.
- SALSTEIN D. A., ROSEN R. D. and PEIXOTO J. P., *J. Atmos. Sci.*, **40** (1983) 788-803.
- SCHOTT F. A., VISBECK M. and SEND U., in *Ocean Processes on Climate Dynamics*, edited by P. MALANOTTE RIZZOLI and A. ROBINSON (Erice, Italy) 1993, pp. 203-225.
- WEARE B. C., NAVATO A. R. and NEWELL R. E., *J. Phys. Ocean.*, **6** (1976) 671-678.
- WOODRUFF S. D., SLEUTZ R. J., JENNE R. L. and STEURER P. M., *Bull. Amer. Meteor. Soc.*, **68** (1987) 1239-1250.
- WU P. and HAINES K., *J. Geophys. Res.*, **101** (1996) 6591-6607.
- WU P. and HAINES K., *J. Geophys. Res.*, **103** (1998) 1121-1131.